Literature Review: Synthesis Methods of NiFe$_2$O$_4$ Nanoparticles for Aqueous Battery Applications

Fatih Izzul Haq[1], Muhammad Aldin Nur Zein[1], Rachel Gabriella[1], Silmi Ridwan Putri[1], Asep Bayu Dani Nandiyanto[1,*], Tedi Kurniawan[2]

[1]Department of Chemical Education, Faculty of Mathematics and Natural Sciences Education, Universitas Pendidikan Indonesia, Jl. Dr. Setiabudi no. 229, Bandung 40154, Jawa Barat, Indonesia
[2]Engineering Technology Departement, Community College of Qatar, Qatar
*Email: nandiyanto@upi.edu

Abstract

Today, the application of NiFe$_2$O$_4$ nanoparticles is increasing in the field of technology that is in great demand, thereby increasing the demand for industrial production. The use of NiFe$_2$O$_4$ nanoparticles can be applied in various technologies, including aqueous batteries. Therefore, an effective method for industrial production is needed. This paper aims to discuss and compare a more efficient method in the synthesis of NiFe$_2$O$_4$. The research method used is a literature review of 62 papers. There are several NiFe$_2$O$_4$ synthesis methods, namely Coprecipitation, Citrate Precursor Technique, Mechanical Alloying, Hydrothermal, Sonochemistry, Reverse Micelle, Sol-Gel, and Pulsed Wire Discharge. The results show that the effective synthesis method of NiFe$_2$O$_4$ is Hydrothermal. This is because the hydrothermal method is economically feasible, environmentally friendly, and has no requirement of high temperatures in the calcination process to produce the final product. The nanoparticle size is around 29.39 nm. This paper is expected to assist in selecting the synthesis method of NiFe$_2$O$_4$.

1 Introduction

Nanotechnology is an active field of scientific research due to its wide range of applications in biology, optics, and electronics. Nanoparticles are of great scientific importance because they are almost a bridge between bulk materials and atomic or molecular structures. The material characteristics change as the size approaches the nanoscale and as the percentage of atoms on the material's surface [1]. One type of nanoparticle is magnetic nanoparticles [2].

Magnetic nanoparticles exhibit a variety of different unique magnetic phenomena. Based on these properties, it can be advantageous for various applications. Magnetic nanoparticles exhibit unique properties and are in great demand in technological applications in ferrofluids, sensors, catalysts, and magnetic resonance imaging (MRI) enhancement. Among them, spinel ferrite crystals have a distinctive structure and high magnetic properties. Such as Nickel ferrite crystals [3]. Among the ferrites that can form the main constituent of magnetic ceramic materials is Nickel ferrite. Nano-sized nickel ferrite has attractive properties for various applications as soft magnets [4].

NiFe$_2$O$_4$ (NFO) has p-type semiconducting material that exists in the inverse spinel structure. Depending on particle size and shape, it exhibits different magnetic properties, such as paramagnetic, superparamagnetic, or ferromagnetic [5]. The research method used in the preparation of this paper is a literature review of 63 journals. Several NiFe2O4 synthesis methods can be used for the synthesis of NiFe$_2$O$_4$ nanoparticles, such as coprecipitation [6], citrate precursors [7], mechanical alloys [8], hydrothermal, sol-gel [9], sonochemical [10], reverse micelle [11], and pulsed wire discharge [12]. Each of the methods has its advantages and disadvantages. Therefore, this paper aims to discuss and compare a more effective method in the synthesis of NiFe$_2$O$_4$. The results show that the effective synthesis method of NiFe$_2$O$_4$ is hydrothermal because the hydrothermal method is economical, environmentally friendly, and does not require high temperatures in the calcination process to produce the final product and the nanoparticle size is around 29.39 nm. This paper is expected to assist in selecting the synthesis method of NiFe$_2$O$_4$.

2   Study of Synthesis Method

Some of the methods used for the synthesis of NiFe$_2$O$_4$nanoparticles can be observed in Table 1. Table 1 shows the methods of synthesizing NiFe$_2$O$_4$ through methods such as coprecipitation [6], citrate precursors [7], mechanical alloys [8], hydrothermal, sol-gel [9], sonochemical [10], reverse micelle [11], and pulsed wire discharge [12].

Table 1 Methods synthesis of NiFe$_2$O$_4$

Methods	Result	Advantages	Disadvantages	Reference
Coprecipitation	The result is a brown powder with a particle size of 18 nm.	The tools used are simple and the costs required are low.	To get better nanoparticles, they must be processed further.	[6]
Citrate Precursor Technique	The resulting particle size is 6.72 - 29.2 nm with a temperature of 523 K - 973K.	The preparation process is simple, the price of the precursor is cheap, and it produces nanometric particles.	The tools used are quite complicated.	[7]
Mechanical Alloying	The resulting particle size is 12-17 nm.	The temperature used can use room temperature, the process is environmentally friendly, and the costs required are low.	The tools used are quite complicated.	[8]
Hydrothermal	The resulting particle size is 29.39 nm at a reaction temperature of 220°C	Environmentally friendly, easy synthesis, does not require calcination at high temperatures to produce the final product.	Must use a sealed container or autoclave in Teflon-coated stainless steel.	[9]
Sonochemical	The particle size produced is on average 9-17 nm at a temperature of 5000 K and a pressure of 20 MPa	Produced nanoparticles < 20 nm in size, much less agglomeration of sonochemically synthesized nanoparticles. A significant reduction in agglomeration can be achieved by increasing the ultrasound intensity and the resulting product is purer and more homogeneous.	The tools used are quite complicated and expensive, the reaction to be the final product at a temperature of about 5000 K and a pressure of 20 MPa	[10]
Reverse Micelle	The resulting particle size ranges from 5-8 nm at the reaction temperature.	Produce nanoparticles measuring <10 nm.	The pH value during synthesis can affect the size and magnetic properties of the synthesized NiFe$_2$O$_4$ nanoparticles.	[11]
Sol-Gel	The resulting particle size is 52.16 nm at a temperature of 500 °C.	The resulting product is purer and more homogeneous.	The temperature used is high, the processing time is long.	[9]
Pulsed Wire Discharge	The resulting particle size is 46 nm at a pressure of 600 Torr with a voltage of 3-6 kV.	High pressure leads to smaller particle size, energy conversion efficiency, and simple equipment.	Less effective for synthesizing intermetallic metals (metal alloys) such as NiAl even at high temperatures.	[12]

3   Synthesis Method of NiFe$_2$O$_4$

Nanocrystalline NiFe$_2$O$_4$ has been synthesized by various methods such as coprecipitation, sonochemical processes, polymer precursor techniques, mechanical alloys, sol-gel, pulsed wire release, shock waves, inverted micelles, hydrothermal, and ultrasonic-assisted hydrothermal processes [6,13].

3.1   Coprecipitation method

The synthesis method of NiFe$_2$O$_4$ nanostructures with various morphologies has been widely developed in physical and chemical methods. The chemical method has advantages over physical methods such as low cost, the reaction at room temperature, and the possibility of large-scale production. The coprecipitation method is suitable for producing reproducible stoichiometric compositions of ferrites withano-sized particles[14].

NiCl$_2$.6H$_2$O dan FeCl$_3$.6H$_2$O were mixed as Ni^{2+} and Fe^{3+} ions providers with a mole fraction ratio of 1:2. The synthesis process was carried out by dissolving 1.188 g of NiCl$_2$.6H$_2$O and 2,701 g FeCl$_3$.6H$_2$O into 20 mL of distilled water [15]. The solution was heated to 40°C and stirred continuously for an exothermic reaction [16]. NiFe$_2$O$_4$ nanoparticles are made by a mixture of hydrated sulfate of iron and Nickel

produced from fly ash [16]. The solution mixture was put into 50 mL of NaOH solution (as a precipitation agent) dropwise slowly while stirring using a magnetic stirrer at 1000 rpm for 60 minutes [15, 18, 19]. The reactants were stirred consistently until the pH level reached 12. Adequate oleic acid was added to the solution as a surfactant. While in [13] the coprecipitation process is carried out by adding a certain amount of polyvinyl pyrrolidone (PVP). Polyvinylpyrrolidone (PVP) is used as a polymer because of its stabilizing ability and can also affect the type of $NiFe_2O_4$ nanostructure. In the process, 0.2 g of polyethylene oxide was added. Next, the solution is heated to 80°C for 30 – 40 minutes[6, 20]. The resulting solution is then placed on a permanent magnet to accelerate precipitation and lower the solution's temperature [6, 15]. The solution was centrifuged and washed 2-7 times. The solution was centrifuged and washed 2-7 times with distilled water and ethanol to remove unwanted impurities and residual surfactant [21]. Then dried for 4 hours at a temperature of 80-100°C. The substance obtained is then ground into a fine powder[6].

In the coprecipitation process to produce $NiFe_2O_4$ nanoparticles, 0.2 M iron nitrate solution (20 mL) and 0.1 M nickel nitrate solution (20 mL) were prepared and mixed with stirring for 1 hour at 80°C. Polyethylene oxide (PEO) is added to the solution as a covering agent. Next, 5 mL of hydrazine hydrate was added dropwise into the solution and a brown precipitate was formed. Finally, the precipitate was separated by centrifugation and dried in a hot air oven for 4 hours at 100 °C [22].

3.2 Citrate precursor technique method

The Citrate Precursor technique is a method with a unique combination of sol-gel method chemicals. It has the advantages of using inexpensive precursors, a simple preparation process, and generating nanometric particles. This technique has been used to prepare different magnetic materials. Samples were characterized by X-ray diffraction (XRD), infrared (IR) spectroscopy, transmission electron microscopy (TEM) [23]. The precursor citrate technique can produce pure and chemically homogeneous nanoparticle powder, and the decomposition of the precursor will lead to the formation of nanocrystalline particles at lower temperatures [24].

A solution of 0.2 M nickel nitrate, citric acid, and ferric nitrate was mixed with a molar ratio of Ni: Fe: Citric Acid = 1:2:2.7. The pH value is maintained in the range of 1.25 – 2.5. The resulting homogeneous solution was refluxed for 15 h at 363 K, which was slowly evaporated on a water bath to form a viscous liquid (gel). To remove the adsorbed water further drying was carried out at 373 K in an oven for 5 h. During the drying process, the gel swells into a fine mass which eventually breaks into brittle flakes. X-ray and hygroscopic precursors of amorphous materials are found in nature. The degree of hydration was found to be dependent on the humidity of the atmosphere. Chemical analysis, nickel-iron citrate precursor gave Ni=8.03%, Fe= 15.20%, H_2O= 4.86%, Citrate= 71.90% which confirmed the stoichiometry as $Ni_3Fe_6O_4(C_6H_6O_7)_8.6H_2O$, and according to the value of calculated, Ni= 7.99%, Fe=15.21%, H_2O= 4.90%, Citrate = 71.89% [7]. With an increase in temperature, an increase in the sharpness of the XRD line indicates the growth of crystal size. The crystal size was determined from the XRD width using the Scherrer method [7]. XRD results are shown in Figure 1.
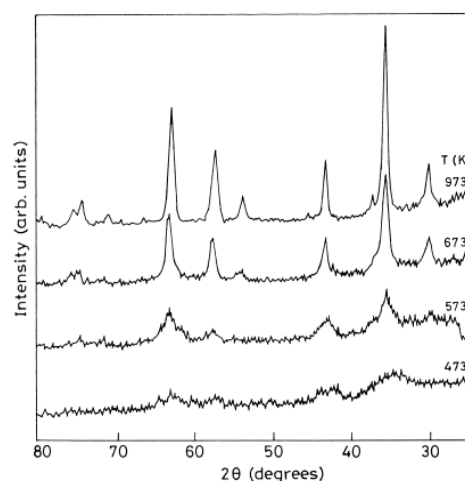

Figure 1 XRD results. Figure adapted from reference [7].

3.3 Mechanical alloys method

The mechanical alloying method has attracted a great deal of interest in recent years, due to its simplicity in the manufacture of a variety of attractive solid materials. Mechanical alloys take advantage of the disturbance of surface-bonded species by pressure to enhance thermodynamic and kinetic reactions at room temperature or at least at temperatures much lower than normally required to produce pure metals. This is due to the energy transferred from the grinding medium to the powder particles, constantly being subjected to cold fracture and welding processes which will determine the final morphology. The synthesized particles usually have a balanced distribution of cations, narrower size distributions, are economically feasible and environmentally friendly [25].

In this method, the magnetic properties and the final structure of the product can be affected by different process parameters such as mill type, milling speed, grinding container, and ball to powder ratio [8]. The $NiFe_2O_4$ synthesis process is illustrated in Figure 2.
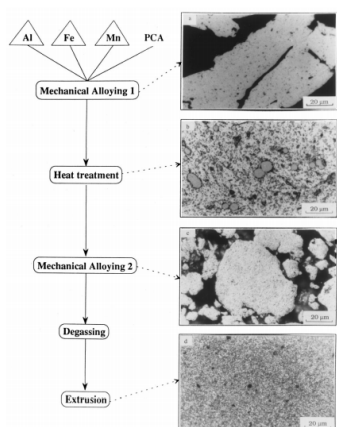
Figure 2 Mechanical alloying method schematic. Figure adapted from reference [8].
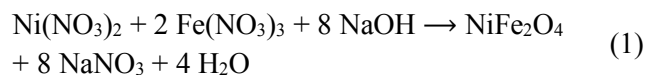
The actual mechanical alloying (MA) process begins with mixing the powder in proper proportions and introducing the powder mixture into the mill along with the grinding medium (generally steel balls). This mixture is then ground for the desired length of time until a steady state is reached when the composition of each powder particle is equal to the proportion of the elements in the initial powder mixture. The milled powder is then consolidated into bulk form and heat-treated to obtain the desired microstructure and properties. Thus the essential components of the mechanical alloying (MA) process are raw materials, factories, and process variables. We will now discuss the various parameters involved in selecting raw materials, type of plant, and process variables [26].

Nickel powder and iron oxide are used as starting materials. To produce $NiFe_2O_4$, NiO, and Fe_2O_3 powders were mixed with a stoichiometric ratio of 1:1 (molar mass). The mechanical activation process is carried out in a high-energy steel ball milling machine. Milling tool characteristics and experimental conditions are described below: Vail (stainless steel, 150 ml volume), ball (stainless steel, five balls 18 mm in diameter), the ball to powder ratio (10:1, 20:1, and 30: 1), atmosphere (argon), milling time (0, 4, 6, 10, 12, 14, 18, 24 and 30 hours). The terms r, R, and as defined above are R = 120 mm, r = 45 mm, dan 150 < < 600 rpm [8].

3.4 Hydrothermal method

The synthesis of $NiFe_2O_4$ nanoparticles can be carried out by the Hydrothermal method. Hydrothermal comes from the word hydro, which means water and thermal, which means heat. So, the hydrothermal method is a method that uses water and heat to convert a solution into crystals. This method must be carried out in a closed system to prevent solvent loss when heated above its boiling point [27]. In general, these methods

require complex synthetic steps, high reaction temperatures, and templates or surfactants [9]. Reaction parameters such as pH, temperature, pressure, and reaction time during hydrothermal synthesis have been shown to play an important role in the synthesized $NiFe_2O_4$ crystal size [19]. The hydrothermal synthesis was carried out in a 1000 mL stainless steel autoclave without stirring. The typical procedure for this synthesis is started by dissolving $NiCl_2 \cdot 6H_2O$, $FeCl_3 \cdot 6H_2O$, and NaOH (ratio 1:2:8) in deionized water. In contrast, NaOH (2 M) is dissolved separately in 30 mL of water and added dropwise with stirring. Constant with the pH of the mixed solution ranging from 8.0 to 10.0 [9,28,29]. NaOH acts as a precipitating agent [30] and uses urea as a precipitating agent [31]. The solution was stirred with a magnetic stirrer for 30 minutes. The reaction is as follows [32] (1).

$$Ni(NO_3)_2 + 2\ Fe(NO_3)_3 + 8\ NaOH \rightarrow NiFe_2O_4 + 8\ NaNO_3 + 4\ H_2O \quad (1)$$

Next, the prepared solution was poured into a Teflon-coated stainless steel autoclave at an ambient temperature of 220°C for 15 hours. After the reaction was completed, the mixture was naturally cooled to room temperature, the brown precipitate was collected with a magnet and washed with water. This washing aims to remove dirt and can also be washed using deionized water and pure ethanol [29]. Finally, the resulting $NiFe_2O_4$ nanoparticles were dried overnight at 90°C [9]. The synthesis scheme is shown in Figure 3. Because the resulting $NiFe_2O_4$ nanoparticles have magnetic properties, wherein magnetic nanoparticles have a strong tendency to agglomerate due to magnetic interactions between particles, to prevent them from being coated by surfactants, also called capping agents, which play a dual role in controlling the shape and size of nanoparticles due to their effect on nucleation and growth kinetics. Paul, et al. used Polyethylene glycol as a surfactant [33]. While Dinkar, et.al stated that glycerol is an effective surfactant to make $NiFe_2O_4$ nanoparticles with the desired magnetic properties with controlled particle sizes [30]. Meanwhile, Chen et al. reported a new hydrothermal route without surfactant using ethylene glycol as a single source precursor [34].
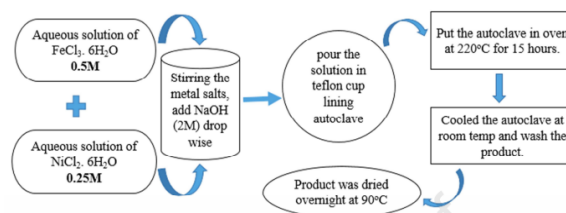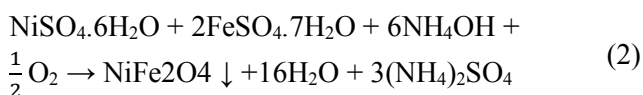

Figure 3 Hydrothermal method schematic. Figure adapted from reference [9].

3.5 Sonochemical method

The sonochemical method utilizes ultrasonic waves in the synthesis reaction of Nickel ferrite nanoparticles. Under certain conditions, most of the acoustic cavitation intensity in ultrasonic waves can be obtained where acoustic cavitation is the process of formation, growth, and rupture of cavities or bubbles in solution [35]. The rupture of a cavity or bubble in the solution will produce a temporary local hot spot with a temperature of 5000 K, a pressure of 1000 atm, and a short time. A good sonochemical process is a volatile precursor because the main sonochemical process is to produce steam in cavitation bubbles. In addition, the vapor pressure of the solvent must be lower at the temperature of the sonochemical process because the vapor of the solvent reduces the efficiency of voiding or bubble bursting [36]. Several phenomena may occur during the administration of ultrasonic radiation. The most prominent effects are a consequence of acoustic cavitation (formation, growth, and bursting of bubbles) and can be categorized as primary sonochemical (gas-phase chemistry occurring inside the collapsing bubble) and secondary sonochemical (solution-phase chemistry occurring outside the bubble) [37]

In the process, nanoparticles were synthesized from 0.4 M $FeCl_3.6H_2O$ and 0,2 M $NiCl_2.6H_2O$ 0,2 precursors with the help of ultrasonic wave radiation. The pH of the solution was changed to 12 by the addition of 3 M NaOH. This reaction occurs at an oxygen pressure of 100-150 kPa (1-1.5 atm). The cavitation process with ultrasonic waves produces a temperature of about 5000 K and a pressure of 20 MPa and produces free radicals H* and OH*. These free radicals form H_2O_2. The oxidizing agent H_2O_2 will oxidize the chloride of iron and Nickel to their respective oxides, forming the final product [10]. More Fe^{3+} ions are reduced to Fe^{2+} by increasing sonication time and power [35]. Higher sonication power and time produces more H* and OH* radicals, which act as reducing agents, thereby increasing the reduction of Fe^{3+} [38]. The sonochemical process uses a sonication flask, which is a probe sonicator (model VC-600, 1,25 cm, 20 kHz, 100 W/cm^2) [36]. After ultrasonic irradiation for 3 hours, the mixture was washed with distilled water, then separated by magnetic centrifugation and dried at 90℃ for 24 hours [39]. The reaction is as follows (2) :
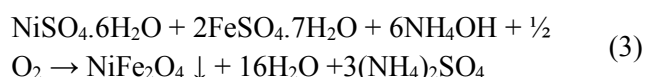
$$NiSO_4.6H_2O + 2FeSO_4.7H_2O + 6NH_4OH + \tfrac{1}{2}O_2 \rightarrow NiFe2O4 \downarrow +16H_2O + 3(NH_4)_2SO_4 \tag{2}$$

The difference in temperature during the mechanical sonication/mixing process results in different hardness of the resulting nanoparticles [40].

3.6 Reverse Micelle method

Another way to make $NiFe_2O_4$ nanoparticles with nanometer size is the reverse micelle method. Micelle is a hollow colloidal particle that is generally a self-assembly organic material [41]. Reverse Micelle is a nano-sized water droplet present in a micro-emulsion with a certain composition. It is known to be an excellent medium for the synthesis of nanoparticles with uniform morphology [42]. Reverse micelles can be formed when surfactants are dissolved in organic solvents. They form both in the presence and in the absence of water. If the medium is entirely free of water, the crystal aggregates are very small and polydispersity. When water is present, it readily dissolves in the polar core, forming so-called 'water pools' which are characterized by a water-surfactant molar ratio. Aggregates containing a small amount of water ([w]/[s]<15) are called reverse micelles, whereas microemulsions correspond to droplets containing a large number of water molecules ([w]/[s] > 15) [43].

In the reverse micelle technique, two microemulsion systems are used. The first microemulsion system is an oil phase microemulsion consisting of isooctane and sodium dioctyl sulfosuccinate (AOT) and the second is an aqueous phase emulsion consisting of isooctane and diisooctyl sulfosuccinate with a reactant salt. In a typical experiment, microemulsion I consisted of 2 ml 30%, 2,4 ml H_2O, 66 ml AOT/iso-octane 0,5 M, and microemulsion II contained 0,384 g $FeSO_4.7H_2O$, 0,192 g $NiSO_4.6H_2O$, 66 ml 0,5 M AOT/iso-octane. NH_4OH b acts as a precipitating agent to form metal hydroxides and also provides stability to water-in-oil systems. The two micro-emulsions were mixed and subjected to rapid mechanical stirring for 50 min. Nickel and iron hydroxides are deposited in a Reverse Micelle pool of water and then oxidized to nickel ferrite. The resulting nickel ferrite was separated by centrifugation, washed with methanol, followed by drying in a low vacuum at 300℃. The ferrite produced by the Reverse Micelle method is hereinafter referred to as the RM compound [44]. Precipitation of nickel ferrite occurs according to the following reaction [11] (3):
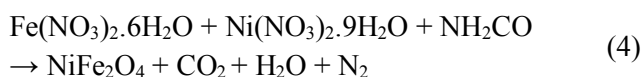
$$NiSO_4.6H_2O + 2FeSO_4.7H_2O + 6NH_4OH + \tfrac{1}{2}O_2 \rightarrow NiFe_2O_4 \downarrow + 16H_2O +3(NH_4)_2SO_4 \tag{3}$$

3.7 Sol-gel method

The synthesis of $NiFe_2O_4$ can be carried out in several stages. The first is to dissolve iron nitrate with 50 mL of a 0.2 M CH_3COOH solution at a temperature of 65℃, then add to the solution yttrium oxide which has been dissolved with 50 mL of Nickel nitrate, which has been dissolved in water. Stirred for one hour at the

same temperature. The next step is the addition of 2 mL of ethylene glycol as a complex agent. Then a transparent brown gel will be formed, which is then dried at a temperature of 110°C. After drying, the gel was powdered and heated at 800°C for 2 hours. In the final stage, calcination is carried out at a temperature of 1000°C for 10 hours [45].

The sol-gel method for synthesizing $NiFe_2O_4$ prepared a solution of Ferric nitrate $Fe(NO_3)_2$ and Nickel nitrate $Ni(NO_3)_2$ in a ratio of 1:2. They were then dissolved in ethylene glycol at a temperature of 40°C. Heating is carried out to a temperature of about 60°C so that a wet gel is formed. The dry gel will be formed when heating at a temperature of 100°C [4]. The formation of a transparent sol can be done by mixing a solution of Ferric nitrate $Fe(NO_3)_2$ and Nickel nitrate $Ni(NO_3)_2$ then mixed with a solution of Polyacrylic Acid (PAA), then stirred slowly until a transparent green solution is formed [46]. The solution was heated to a temperature of 60°C until a transparent sol was formed, adding urea to the iron and nickel nitrate solution in a ratio of 2.22, and heating was carried out on a magnetic stirrer until all the H_2O evaporated. The wet viscous gel was transferred to a porcelain dish and heated for 4 hours at 400°C to produce $NiFe_2O_4$ crystalline powder [3]. The burning powder is a small amount of Nickel ferrite directly formed after combustion. The change in the nickel ferrite crystals from the gel is due to the heat generated and the exothermic reaction of nitrate and citric acid. Thus, the following reaction occurs [47] (4):

$$Fe(NO_3)_2.6H_2O + Ni(NO_3)_2.9H_2O + NH_2CO \quad (4)$$
$$\rightarrow NiFe_2O_4 + CO_2 + H_2O + N_2$$

The addition of citric acid to a solution of Iron nitrate and Nickel nitrate makes the reaction atmosphere in an acidic state [48]. The citric acid in a 1:1 ratio [49]. The addition of citric acid is to accelerate the formation of metal ion chelates. Then the citric acid solution was neutralized by adding 30% ammonia solution to pH 7. In addition to citric acid and urea as chelating agents, Polyvinyl Alcohol (PVA) can also be used as a chelating agent, but it is insoluble in water at room temperature [50]. Polyvinyl Alcohol (PVA) is soluble in water at a temperature of 50°C. The results of the XRD graph are shown in Figure 4. The calcined phase will be identified by X-ray (XRD). The XRD pattern graph of the sol-gel method above reveals the amorphous nature of $NiFe_2O_4$ and can be compared with the XRD graph of the Joint Committee on Powder Diffraction Standard (JCPDS file no 10-325), which shows that the crystal structure of $NiFe_2O_4$ is a cubic spinel crystal [51]. Meanwhile, to measure the crystal size, the Scherrer formula was used and the results

obtained that the particle size of $NiFe_2O_4$ was 52.16 nm [9].
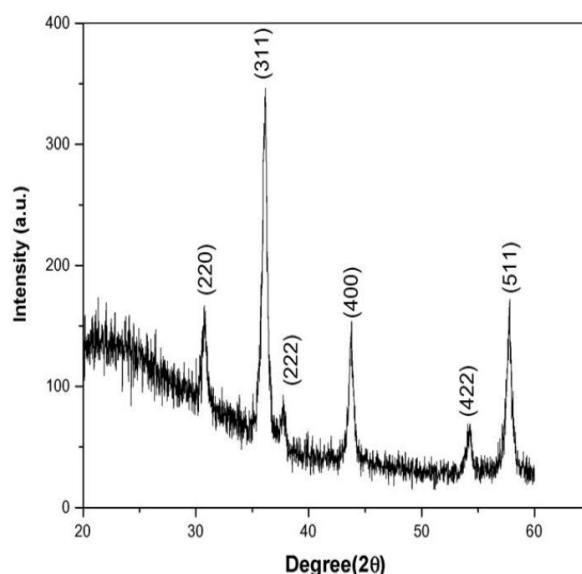

Figure 4. XRD Graph of Sol-Gel Method. Figure adapted from reference [51].

3.8   Pulsed wire discharge method

Synthesizing nanoparticles with physical processes is limited by several factors, including system scale, operational and maintenance costs. In a physical process, the material must be heated for evaporation to occur. For some materials, this requires very high temperatures, where ordinary heating will not be effective [52]. In addition to metal particles formed by this method, in an inert gas atmosphere, it is possible to synthesize oxide, nitride, and carbide particles in a suitable reactive gas atmosphere. In this way, many types of wire have been used to form nano-sized particles [53]. The Pulsed Wire Discharge method is a unique process in that high-density plasma can easily transmit high currents through thin wires. This method can be used for the synthesis of nanoparticles [54]. The basic principle of nanoparticle synthesis by the Pulsed Wire Discharge method is shown in Figure 5.
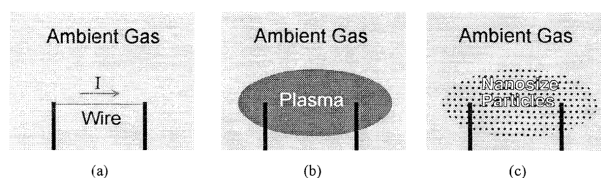

Figure 5 Basic Schematic of Pulsed Wire Discharge Method. Figure adapted from reference [53].

An electric current is passed through a solid wire located in the middle of the gas (ambient gas). Electrical energy from the current source is stored in the wire because of its limited resistance. This stored energy causes the wire to melt, vaporize and ionize the

wire material, resulting in a plasma expanding around the gas. This high-temperature plasma slowly cools due to interactions with the surrounding gases that produce vapor from the wire material. The resulting vapor then condenses around the gas [55]. Changes in plasma and vapor during the Pulsed Wire Discharge process are observed with a high-speed camera through a response spectrum that appears around 400 to 900 nm [56].

The wire is placed between the electrodes in the tube chamber. After the vacuum pump-out is rotated, the tube chamber is filled with gas at a pressure of 100 kPa. The current capacitor has a voltage of 6 kV with a high DC voltage. The wire heats up, evaporates, and forms plasma due to the high current flowing. The nanoparticles will collect on the surface of the filter membrane [57]. A membrane filter is installed between the chamber and a rotary pump which functions to collect the powder. When the voltage switch is released, the photodetector responds to the current and triggers the high-speed camera to start recording [56].

The construction of the Pulsed Wire Discharge equipment is shown in Figure 6. The apparatus consists of a discharge circuit and a wire feed chamber. The metal wire is wound onto coils in the production chamber (chamber). A machine operates the wire feeding chamber (chamber) with a wire holder. The machine is controlled by a PC and machine control unit. The discharge circuit consists of a charger, a capacitor bank, a switch, and electrodes [58].
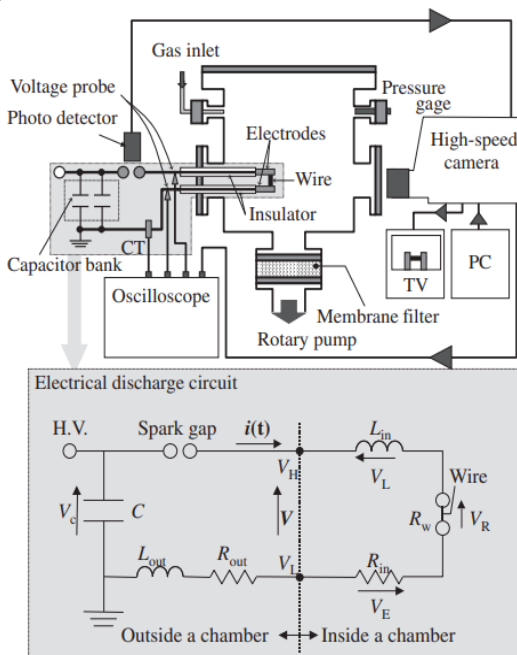

Figure 6 Schematic of Pulsed Wire Discharge Method. Figure adapted from reference [58].

A high current is passed through Nickel and Iron wire, with a length of 25 mm. the wires are connected to electrodes in a chamber filled with oxygen gas at a pressure of 100 to 600 torr. The electrodes are connected to a current source via a switch. The current source or capacitor has a voltage of 3-6 kV. The wire will evaporate due to heat and turn into plasma. Plasma will evaporate and slowly cool down due to interaction with gases around the room [12]. Only the wire between the electrodes is heated, evaporated, and converted into plasma [59]. The wires are simultaneously energized in a chamber filled with oxygen. After that, the powder particles will float in the area around the gas in the room. Then the powder will be collected by pumping the gas through a 0.1-micrometer porous membrane. Emissions from the process can be observed directly through a window with high-speed photography. The results of the recording of high-speed photography equipment observed through the chamber window with a time interval of about 0 to 120 microseconds are shown in Figure 7.
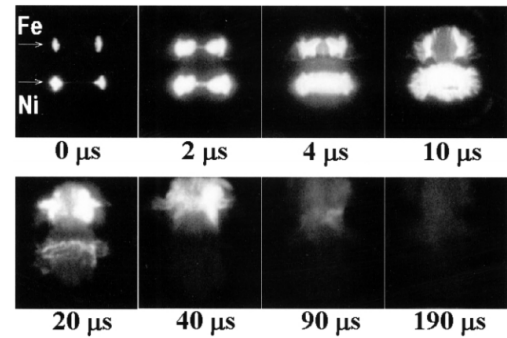

Figure 7 Recording Results of High-Speed Photography Equipment. Figure adapted from reference [60].

4 Synthesis Results

In the $NiFe_2O_4$ synthesis process by coprecipitation method, the resulting phase is identified by X-ray (XRD). The diffraction pattern formed shows an indication of the formation of the $NiFe_2O_4$ phase marked by the peak of the plane. The grain size of the synthesized $NiFe_2O_4$ nanoparticles decreased with increasing NaOH concentration. This is predicted to happen because NaOH is a good decomposer. The grain size of synthesized $NiFe_2O_4$ nanoparticles can also increase with increasing synthesis temperature. This occurs because the increase in the synthesis temperature causes an increase in the growth activity of nanoparticles due to thermal effects during the synthesis process [15]. While [6] XRD patterns of $NiFe_2O_4$ nanoparticles were recorded using a powder X-ray diffractometer, with diffraction angles between 30° and 60°. The pattern indicates the formation of a single-phase cubic crystal structure. The average

crystal size of the sample can be calculated using the Scherrer formula, and the result is 18 nm. While synthesizing $NiFe_2O_4$ using the citrate precursor method, the XRD pattern for the samples was heat-treated at various temperatures. The amorphous spinel phase is formed at about 473 K, which crystallizes entirely above 553 K. The broad peak indicates the absence of crystal periodicity. For the 573 K sample, the lattice parameter, a = b = c = 8.4372 Å was larger than the reported value of 8.3390 λ compared to bulk particles or well-crystallized samples. This shows the lattice expansion and the smaller particle size of the spinel ferrite $NiFe_2O_4$ [7].

In the $NiFe_2O_4$ synthesis process by mechanical alloy method, an X-ray diffraction spectrometer (XRD) was used to analyze the phase change during the ball milling process. The Bragg diffraction angle (2θ) was selected in the range of 20° - 80° and Cu Kα λ = 0.154 nm was applied. Since crystal size and lattice strain are the most important factors affecting properties such as microstructure and magnetic properties, it was decided to use the modified Scherrer equation [8].

In the $NiFe_2O_4$ synthesis process using the hydrothermal method, XRD analysis was carried out to analyze the structural properties of $NiFe_2O_4$. The XRD pattern shows (2 2 0), (3 1 1), (2 2 2), (4 0 0), (4 2 2) (5 1 1), (4 4 0) and (5 3 3) , which correlates with the cubic spinel structure. This peak reveals the formation of the pure form of $NiFe_2O_4$. The XRD pattern of Nickel ferrite with the hydrothermal method has a sharp peak which indicates good crystallinity. All NiFe2O4 diffraction peaks match (JCPDS file no. 10-325). The crystal size can be calculated using the Full-Width Half Maximum (FWHM) and the Scherrer formula [9,61]. Thus, the average crystal size of NiFe2O4 is 29.39 nm.

Meanwhile, Scanning Electron Microscopy (SEM) with an absorption band of 100-1000 cm^-1 can determine the morphological form of NiFe2O4 crystals, which are semi-spherical. By using a vibrating sample magnetometer (VSM) can measure the magnetic properties of ferrite $NiFe_2O_4$. $NiFe_2O_4$ ferrite exhibits higher saturation magnetization while low coercivity, which is due to its high crystallinity and uniform morphology $NiFe_2O_4$ ferrite made by hydrothermal method showed saturation magnetization (Ms) and coercivity (Hc) values of 48,63 emug^-1 and 77,70 Oe [7]. Scanning electron microscopy (SEM) with an acceleration voltage of 20 kV can also be used to test the morphology of the sample and its microstructure [62].
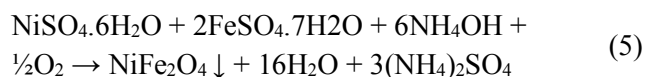
Analysis using XRD and TEM (Transmission electron microscope) showed that increasing reaction temperature, holding time, and RH ratio would promote the evolution and crystallization of $NiFe_2O_4$ nanoparticles. Good quality Ni-ferrite powder with nanometer size and perfect morphology can be easily synthesized by appropriately adjusting processing factors under hydrothermal process [29].

In the $NiFe_2O_4$ synthesis process using the sonochemical method, the synthesized NiFe2O4 nanoparticles were studied for their crystal structure and size using X-Ray Diffraction Powder (PXRD). The analyzed $NiFe_2O_4$ samples were milled manually in a mortar, then placed on the flat side of the sample holder and measurements were made; the scan step size is 0.02° and the integration time is 0.6 s/step. The PXRD patterns used are (220), (311), (222), (400), (422), (511) and (440) associated with values of 2Θ 30.4°, 35.7°, 38.0, 43.5, 54.1, 57.5, and 63.1°. The result is that the crystal structure of $NiFe_2O_4$ is face-centered cubic (FCC) according to the standard reference (JCPDS Card No.10-0325). The secondary phase, hematite (α-Fe2O3) was observed at 2Θ values of 33.4, 40.9, and 49.6 (JCPDS Card No: 79-0007), while the synthesized crystal size ranged from 9 to 17 nm [10].

Nanocrystalline nickel ferrite synthesized by the Reverse Micelle technique was characterized by high-resolution transmission electron microscopy (TEM), X-ray diffraction (XRD) technique, and its magnetic behavior could be studied by a superconducting quantum interference device (SQUID). Two different kinds of measurements can carry out measurement of magnetic properties with SQUID: (a) zero-field cooling (ZFC) and field-cooled magnetization (FC) versus temperature measurement and (b) magnetization as a function of the applied field [41].

Precipitation of nickel ferrite occurs according to the following reaction [11] (5):

$$NiSO_4.6H_2O + 2FeSO_4.7H2O + 6NH_4OH + \tfrac{1}{2}O_2 \rightarrow NiFe_2O_4 \downarrow + 16H_2O + 3(NH_4)_2SO_4 \qquad (5)$$

The experimental results using TEM showed that the $NiFe_2O_4$ particle size was about 5-8 nm, while the XRD results with a wavelength of Cu = 1,54 λ gave an average crystal size of about 3 nm. The SQUID results showed magnetic properties at 300 K (room temperature) is 25.4 emu/g and at 2K 35.5 emu/g. The crystal size obtained for nickel ferrite by reverse micelle technique is significantly smaller than that obtained by ball milling, hydrolysis, chemical precursor technique, sol-gel technique, and sonochemical method [11]. This can happen because the pH value during synthesis can affect the size and

magnetic properties of the synthesized $NiFe_2O_4$ nanoparticles [42].

In the $NiFe_2O_4$ synthesis process using the sol-gel method, the calcined phase will be identified by X-ray (XRD), as shown in Figure 8 [36]. The XRD pattern graph of the sol-gel method reveals the amorphous nature of $NiFe_2O_4$ and can be compared with the XRD graph of the Joint Committee on Powder Diffraction Standard (JCPDS file no 10-325) [50]. The sample represents a cubic structure with a space group of Fd-3m. based on data analysis on XRD, no second phase is formed. This indicates the formation of the desired product at a temperature of 500°C [3]. Meanwhile, to measure the crystal size, the Scherrer formula was used and the results obtained that the particle size of $NiFe_2O_4$ was 52.16 nm [9].
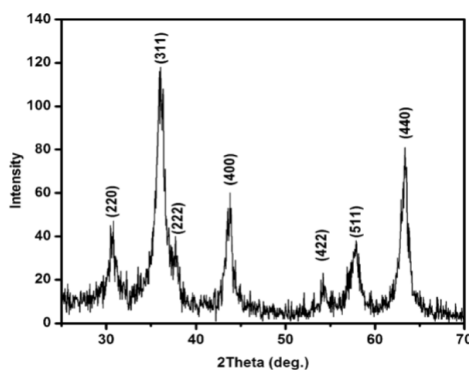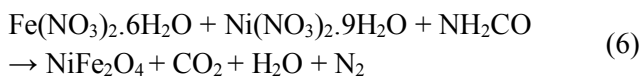

Figure 8 Graph of XRD Results for Synthesis of $NiFe_2O_4$ with Sol-Gel Method. Figure adapted from reference [36]

From the XRD data analysis results, it can be said that after the calcination stage in the sol-gel method, $NiFe_2O_4$ has been formed. The reaction is as follows [48] (6):

$$Fe(NO_3)_2.6H_2O + Ni(NO_3)_2.9H_2O + NH_2CO \rightarrow NiFe_2O_4 + CO_2 + H_2O + N_2 \tag{6}$$

In synthesizing NiFe2O4 with the pulsed wire discharge method, it is possible to observe the resulting images from high-speed camera recordings that capture the light spectrum. The light can be observed about 5-8 microseconds after opening the current switch. Emissions from Ni wire appear earlier than Fe. As a result, the wire with the lower resistance heats up faster. The resistance of the Ni wire is estimated to be half that of the Fe wire [60].

The XRD graph was obtained from the synthesis of $NiFe_2O_4$, which was processed at a pressure of 600 Torr of oxygen gas and can be compared with the XRD graph of the Joint Committee on Powder Diffraction Standard. At a pressure of 600 Torr, the particle size results in the range of 46 nm. The results of the XRD graph are shown in Figure 9.
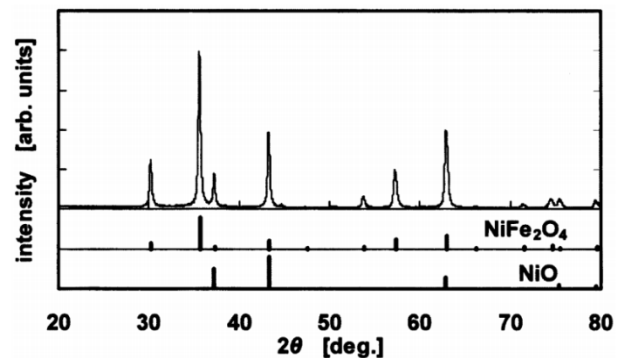

Figure 9 XRD graph results for the synthesis of $NiFe_2O_4$ Pulsed Wire Discharge method. Figure adapted from reference [12]

5 Conclusion

Several methods that can be used for the synthesis of $NiFe_2O_4$ nanoparticles include the method coprecipitation [6], citrate precursors [7], mechanical alloys [8], hydrothermal, sol-gel [9], sonochemical [10], reverse micelle [11], and pulsed wire discharge [12]. The results show that the effective synthesis method of $NiFe_2O_4$ is Hydrothermal. This is because the hydrothermal method is economical, environmentally friendly, and does not require high temperatures in the calcination process to produce the final product. The nanoparticle size is around 29.39 nm.

References

[1] Z. K. Karakas, R. Boncukcuoglo, I. H. Karakas, "The effects of fuel type in synthesis of $NiFe_2O_4$ nanoparticles by microwave assisted combustion method," *J. Phys.*, vol. 707, no. 1, p. 012046, 2016.

[2] Y. Pourshojaei, F. Zolala, K. Eskandari, M. Talebi, L. Morsali, M. Amiri M, et al., "Nickel ferrite ($NiFe_2O_4$) nanoparticles as magnetically recylable nanocatalyst for highly efficient synthesis of 4h-chromene derivatives," *J. Nanosci. Nanotechnol.*, vol. 20, no. 5, pp. 3206-3216, 2020.

[3] R. Sen, P. Jain, R. Patidar, S. Srivastava, R. S. Rana, N. Gupta, "Synthesis and characterization of nickel ferritte ($NiFe_2O_4$) nanoparticles prepared by sol-gel method," *Mater. Today: Proc.*, vol. 2, no. 2015, pp. 3750-3757, 2015.

[4] M. George, A. M. John, S. S. Nair, P. A. Joy, M. R. Anantharaman, "Finite size effect on the structural and magnetic properties of sol-gel synthesized $NiFe_2O_4$ powders," *J. Magn. Magn. Mater.*, vol. 302, no. 2006, pp. 190-195, 2006.

[5] T. D. Dongale, S. S. Khot, A. A. Patil, S. V. Wagh, P. B. Patil dan D. P. K. T. G. Dubal, "Bifunctional nanoparticulated nickel ferrite thin films: Resistive memory and aqueous battery applications," *Mater. Des.*, vol. 201, p. 109493, 2021.

[6] S. Sagadevan, Z. Z. Chowdhyr, R. F. Rafique, "Preparation and characterization of nickel ferrite nanoparticles via co-precipitation method," *Mater. Res.*, vol. 21, no. 2, 2018.

[7] S. Prasad, N. Gajbhiye, "Magnetic studies of nanosized nickel ferrite particles synthesized by the citrate precursor technique," *J. Alloys Compd.*, vol. 265, no. 1-2, pp. 87-92, 1998.

[8] A. Hajalilou, M. Hashim, R. Ebrahimi-Kahrizsangi, Mohamed Kamari H, Kanagesan S. "Parametric optimization of $NiFe_2O_4$ nanoparticles synthesized by mechanical alloying," *Mater. Sci.-Pol.*, vol. 32, no. 2, pp. 281-291, 2014.

[9] F. Majid, J. Rauf, S. Ata, I. Bibi, A. Malik, S. M. Ibrahim, et al., "Synthesis and characterization of $NiFe_2O_4$ ferrite: Sol-gel and hydrothermal synthesis routes effect on magnetic, structural and dielectric characteristics," *Mater. Chem. Phys.*, 2020; 258: 123888.

[10] M. A. S. Amulya, H. P. Nagaswarupa, M. R. A. Kumar, C. R. Ravikumar, S. C. Prashantha, K. B. Kusuma, "Sonochemical synthesis of $NiFe_2O_4$ nanoparticles: Characterization and their photocatalytic and electrochemical applications," *Appl. Surf. Sci.*, vol. 1, no. 100023, 2020.

[11] A. Kale, S. Gubbala, R. D. K. Misra, "Magnetic behavior of nanocrystalline nickel ferrite synthesized by the reverse micelle technique," *J. Magn. Magn. Mater.*, vol. 273, no. 3, pp. 350-358, 2004.

[12] P. Y. Lee, K. Ishizaka, H. Suematsu, "Magnetic and gas sensing property of nano-sized $NiFe_2O_4$ powders synthesized by pulsed wire discharge," *J. Nanoparticle Res.*, vol. 8, no. 2006, pp. 29-35, 2006.

[13] P. Sivakumar, R. Ramesh, A. Ramanand, S. Ponnusamy, C. Muthamizhchelvan, "Synthesis and characterization of $NiFe_2O_4$ nanosheet via polymer assited co-precipitation method," *Mater. Lett.*, vol. 65, no. 3, pp. 483-485, 2011.

[14] S. S. Jadhav, S. E. Shirsath, B. G. Toksha, S. M. Patange, D. R. Shengule, K. M. Jadhav, "Structural and electric properties of zinc substituted $NiFe_2O_4$ nanoparticles prepared by co-precipitation method," *Phys. Rev. B Condens. Matter.*, vol. 405, no. 12, pp. 2610-2614, 2010.

[15] M. Muflihatun, S. Shofiah, E. Suharyadi, "Sintesis nanopartikel nickel ferrite ($NiFe_2O_4$) dengan metode kopresipitasi dan karakteristik sifat kemagnetannya," *J. Fis. Indones.*, vol. 19, no. 55, pp. 20-25, 2015.

[16] E. Agouriane, A. Essoumhi, A. Razouk, M. Sahlaoui, M. Sajieddine, "X-ray diffraction and Mössbauer studies of $NiFe_2O_4$ nanoparticles obtained by co-precipitation method," *J. Mater. Environ. Sci.*, vol. 7, no. 12, pp. 4614-4619, 2016.

[17] K. S. Abdel-Halim, M. Bahgat, O. A. Fouad, "Thermal synthesis of nanocrystalline FCC Fe-Ni alloy by gaseous reduction of coprecipitated $NiFe_2O_4$ from secondary resources," *Mater. Sci. Technol.*, vol. 22, no. 12, pp. 1396-1400, 2006.

[18] J. Li, Y. Lin, X. Liu, Q. Zhang, H. Miao, T. Zhang, et al, "The study of transition on $NiFe_2O_4$ nanoparticles prepared by co-precipitation/calcination," *Phase Transit.*, vol. 84, no. 1, pp. 49-57, 2011.

[19] N. Gupta, P. Jain, R. Rana, S. Shrivastava, "Current development in synthesis and characterization of nickel ferrite nanoparticles," *Mater. Today: Proc.*, vol. 4, no. 2, pp. 342-349, 2017.

[20] R. Zandipak, S. Sobhanardakani, "Synthesis of $NiFe_2O_4$ nanoparticles for removal of anionic dyes from aqueous solution," *Desalin. Water Treat.*, vol. 57, no. 24, pp. 11348-11360, 2015.

[21] M. Aliahmad, M. Noori, K. N. Hatefi, M. Sargazi, "Synthesis of nickel ferrite nanoparticles by co-precipitation chemical method," *Int. J. Phys. Sci.*, vol. 8, no. 18, pp. 854-858, 2012.

[22] P. Sivakumar, R. Ramesh, A. Ramanand, S. Ponnusamy, C. Muthamizhchelvan, "Synthesis and characterization of $NiFe_2O_4$ nanoparticles and nanorods," *J. Alloys Compd.*, vol. 563, pp. 6-11, 2013.

[23] C. L. A. Gracia, S. M. Montemayo, "Synthesis of $CoFe_2O_4$ nanoparticles embedded in a silica matrix by the citrate precursor technique," *J. Magn. Magn. Mater.*, vol. 294, no. 2, pp. 43-46, 2005.

[24] N. Yang, H. Yang, J. Jia, X. Pang, "Synthesis of $CoFe_2O_4$ nanoparticles embedded in a silica matrix by the citrate precursor technique," *J. Magn. Magn. Mater.*, vol. 438, no. 1-2, pp. 263-267, 2007.

[25] S. B. Waje, M. Hashim, W. D. W. Yusoff, Z. Abbas, "X-ray diffraction studies on crystallite size evolution of $CoFe_2O_4$ nanoparticles prepared using mechanical alloying and sintering," *Appl. Surf. Sci.*, vol. 256, no. 10, pp. 3122-3127, 2010.

[26] C. Suryanarayana, "Mechanical alloying and milling," *Prog. Mater. Sci.*, vol. 46, no. 1-2, pp. 1-184, 2001.

[27] K. Byrappa, T. Adschiri, "Hydrothermal technology for nanotechnology," *Prog. Cryst. Growth Charact. Mater.*, vol. 53, no. 2, pp. 117-166, 2007.

[28] V. A. Samson, S. B. Bernadsha, R. Xavier, C. S. T. Rueshwin, S. Prathap, J. Madhavan, et al., "One pot hydrothermal synthesis and characterization of $NiFe_2O_4$," *Mater. Today: Proc.*, 2020.

[29] J. Zhou, J. Ma, C. Sun, L. Xie, Z. Zhao, H. Tian, et al., "Low-temperature synthesis of $NiFe_2O_4$ by a hydrothermal method," *J. Am. Ceram. Soc.*, vol. 88, no. 12, pp. 3535-3537, 2005.

[30] D. K. Dinkar, B. Das, R. Gopalan, B. S. Dehiya, "Effects of surfactant on the structural and magnetic properties of hydrothermally synthesized $NiFe_2O_4$ nanoparticles," *Mater. Chem. Phys.*, vol. 218, pp. 70-76, 2018.

[31] M. Safaei, H. Beitollahi, M. R. Shishehbore, "Synthesis and characterization of $NiFe_2O_4$ nanoparticles using the hydrothermal method as magnetic catalysts for electrochemical detection of norepinephrine in the presence of folic acid," *J. Chin. Chem. Soc.*, vol. 66, no. 12, pp. 1597-1603, 2019.

[32] A. A. Sattar, H. M. EL-Sayed, I. ALsuqia, "Structural and magnetic properties of $CoFe_2O_4/NiFe_2O_4$ core/shell nanocomposite prepared by the hydrothermal method," *J. Magn. Magn. Mater.*, vol. 395, pp. 89-96, 2015.

[33] B. Paul, D. D. Purkayastha, S. S. Dhar, "Size-controlled synthesis of $NiFe_2O_4$ nanospheres via a PEG assisted hydrothermal route and their catalytic properties in oxidation of alcohols by periodic acid," *Appl. Surf. Sci.*, vol. 370, pp. 469-475, 2016.

[34] L. Chen, H. Dai, Y. Shen, J. Bai, "Size-controlled synthesis and magnetic properties of $NiFe_2O_4$ hollow nanospheres via a gel-assistant hydrothermal route," *J. Alloys Compd.*, vol. 491, no. 1-2, pp. 33-38, 2010.

[35] S. I. Liba, M. Tariq, H. N. Das, A. Nahar, S. M. Hoque, "Effect of sintering treatment on the microstructure of $NiFe_2O_4$ synthesized by the sonochemical method and the conventional method," *AIP Adv.*, vol. 10, no. 6, p. 065103, 2020.

[36] K. V. Shafi, Y. Koltypin, A. Gedanken, R. Prozorov, J. Balogh, J. Lendvai, et al., "Sonochemical preparation of nano-sized amorphous $NiFe_2O_4$ particles," *J. Phys. Chem. B.*, vol. 101, no. 33, pp. 6409-6914, 1997.

[37] H. Xu, B. W. Zeiger, K. S. Suslick, "Sonochemical synthesis of nanomaterials," *Chem. Soc. Rev.*, vol. 42, no. 7, pp. 2555-2567, 2013.

[38] S. R. Yousefi, O. Amiri, M. Salavati-Niasari, "Control sonochemical parameter to prepare pure $Zn0.35Fe2.$ $65O_4$ nanostructures and study their photocatalytic activity," *Ultrason. Sonochemistry*, vol. 58, p. 104619, 2019.

[39] Y. Slimani, B. Unal, M. A. Almessiere, A. D. Korkmaz, S. E. Shirsath, G. Yasin, et al., "Investigation of structural and physical properties of Eu^{3+} ions substituted $Ni0.4Cu0.2Zn0.4Fe_2O_4$ spinel ferrite nanoparticles prepared via sonochemical approach," *Results Phys.*, vol. 17, p. 103061, 2020.

[40] H. Nathani, S. Gubbala, R. D. K. Misra, "Magnetic behavior of nanocrystalline nickel ferrite: Part I. The effect of surface roughness," *Mater. Sci. Eng. B.*, vol. 121, no. 1-2, pp. 126-136, 2005.

[41] M. Abdullah , N. Y. Virgus, Khairurrijal, "Review: sintesis nanomaterial," *J. Nanosci. Nanotechnol.*, vol. 1, no. 2, pp. 33-57, 2008.

[42] S. Thakur, S. C. Katyal, M. Singh, "Structural and magnetic properties of nano nickel–zinc ferrite synthesized by reverse micelle technique," *J. Magn. Magn. Mater.*, vol. 321, no. 1, pp. 1-7, 2009.

[43] R. D. K. Misra, S. Gubbala, A. Kale, W. F. Egelhoff Jr., "A comparison of the magnetic characteristics of nanocrystalline Nickel, zinc, and manganese ferrites synthesized by reverse micelle technique," *Mater. Sci. Eng. B.*, vol. 111, no. 2-3, pp. 164-174, 2004.

[44] K. M. Reddy, L. Satyanarayana, S. V. Manorama, R. D. K. Misra, "A comparative study of the gas sensing behavior of nanostructured nickel ferrite synthesized by hydrothermal and reverse micelle techniques," *Mater. Res. Bull.*, vol. 39, no. 10, pp. 1491-1498, 2004.

[45] A. Gatelytė, D. Jasaitis, A. Beganskienė, A. Kareiva, "Sol-gel synthesis and characterization of selected transition metal nano-ferrites," *Mater. Sci.*, vol. 17, no. 3, pp. 302-307, 2011.

[46] D. H. Chen, X. R. He, "Synthesis of nickel ferrite nanoparticles by sol-gel method," *Mater. Res. Bull.*, vol. 36, no. 7-8, pp. 1369-1377, 2001.

[47] J. Azadmanjiri, S. S. Ebrahimi, H. K. Salehani, "Magnetic properties of nanosize $NiFe_2O_4$ particles synthesized by sol–gel auto combustion method," *Ceram. Int.,* vol. 33, no. 8, pp. 1623-1625, 2007.

[48] J. Mantilla, L. L. Félix, M. A. Rodriguez, F. H. Aragon, P. C. Morais, J. A. H. Coaquira, et al., "Washing effect on the structural and magnetic properties of $NiFe_2O_4$ nanoparticles synthesized by chemical sol-gel method," *Mater. Chem. Phys.,* vol. 213, pp. 295-304, 2018.

[49] P. Lavela, J. L. Tirado, "$CoFe_2O_4$ and $NiFe_2O_4$ synthesized by sol–gel procedures for their use as anode materials for li-ion batteries," *J. Power Sources*, vol. 172, no. 1, pp. 379-387, 2007.

[50] B. V. Prasad, K. V. Ramesh, A. Srinivas, "Structural and magnetic properties of nanocrystalline nickel ferrite ($NiFe_2O_4$) synthesized in sol-gel and combustion routes," *Solid State Sci.*, vol. 86, pp. 86-97, 2018.

[51] M. Srivastava, A. K. Ojha, S. Chaubey, A. Materny, "Synthesis and optical characterization of nanocrystalline $NiFe_2O_4$ structures," *J. Alloys Compd.*, vol. 481, no. 1-2, pp. 515-519, 2009.

[52] W. K. Y. Jiang, "Pulsed wire discharge for nanosized powder synthesis," *IEEE Trans. Plasma Sci.*, vol. 26, no. 5, pp. 1498-1501, 1998.

[53] S. Ishihara, H. Suematsu, T. Nakayama, T. Suzuki, K. Niihara, "Nano-sized particles formed by pulsed discharge of powders," *Mater. Lett.*, vol. 67, no. 1, pp. 289-292, 2012.

[54] W. K. Y. Jiang, "Synthesis of nanosized powders by pulsed wire discharge," *Dig. Tech. Pap.,* vol. 1, pp. 214-219, 1997.

[55] W. Jiang, T. Suzuki, H. Suematsu, K. Yatsui, "Industrial applications of pulsed wire discharge," *in 14th IEEE International Pulsed Power Conference (IEEE Cat. No. 03CH37472)*, pp. 433-436, 2003.

[56] Y. Tokoi, H. B. Cho, T. Suzuki, T. Nakayama, H. Suematsu, K. Niihara, "Particle size determining equation in metallic nanopowder preparation by pulsed wire discharge," *Jpn. J. Appl. Phys.*, vol. 52, no. 5R, p. 055001, 2013.

[57] Y. Tokoi, T. Suzuki, T. Nakayama, H. Suematsu, W. Jiang, K. Niihara, "Effect of wire diameter on particle size of metal nano-sized powder prepared by pulsed wire discharge," *J. Jpn. Soc. Powder Powder Metall.,* vol. 55, no. 3, pp. 192-197, 2008.

[58] S. Nishimura, Y. Hayashi, T. Suzuki, T. Nakayama, H. Suematsu, W. Jiang, et al., "Pulsed wire discharge apparatus for mass production of nanosized powders," *Adv. Mat. Res.*, vol. 11, pp. 315-318, 2006.

[59] C. Cho, K. Murai, T. Suzuki, H. Suematsu, W. Jiang, K. Yatsui, "Enhancement of energy deposition in pulsed wire discharge for synthesis of nano-sized powders," *IEEE Trans. Plasma Sci.,* vol. 32, no. 5, pp. 2062-2067, 2004.

[60] Y. Kinemuchi, K. Ishizaka, H. Suematsu, W. Jiang, K. Yatsui, "Magnetic properties of nanosize $NiFe_2O_4$ particles synthesized by pulsed wire discharge," *Thin Solid Films*, vol. 407, no. 1-2, pp. 109-113, 2002.

[61] G. Kesavan, N. Nataraj, S. M. Chen, L. H. Lin, "Hydrothermal synthesis of $NiFe_2O_4$ nanoparticles as an efficient electrocatalyst for the electrochemical detection of bisphenol A," *New J. Chem.,* vol. 44, no. 19, pp. 7698-7707, 2022.

[62] L. Guo, Y. He, D. Chen, B. Du, W. Cao, Y. Lv, et al. "Hydrothermal synthesis and microwave absorption properties of nickel ferrite/multiwalled carbon nanotubes composites," *Coatings*, vol. 11, no. 5, p. 534, 2021.